Nanoscale Devices Based on Two-dimensional Materials and Ferroelectric Materials

Zihan Yao, Hojoon Ryu, Kai Xu, Jialun Liu, Yuhang Cai, Yueming Yan, and Wenjuan Zhu*

Department of Electrical and Computer Engineering, University of Illinois at Urbana-Champaign * Email: wjzhu@illinois.edu

Abstract

In this paper, we review our research on nanoscale electronic and optoelectronic devices based on two-dimensional (2D) materials and ferroelectric materials. Our study reveals that the current transport in graphene is highly influenced by the number of layers, local topography, and gate dielectrics on the graphene. High-performance radio-frequency (RF) devices and plasmonic photodetectors were fabricated based on graphene. We also synthesized monolayer molybdenum disulfide (MoS₂) and tungsten diselenide (WSe₂) using chemical vapor deposition. The domain size of monolayer WSe₂ exceeds 100 μm . We demonstrate that logic devices based on MoS₂ have the potential to suppress short-channel effects and have high critical breakdown electric field. The gap states of MoS₂ were

characterized using ac conductance. We found that the true band mobility of MoS₂ is much higher than the measured effective mobility due to the large number of gap states. In addition, we systematically investigated ferroelectric aluminum (Al)-doped hafnium oxide (HfO₂) with various top electrodes, Hf to Al ratios, and annealing temperatures. High-quality ferroelectric Al-doped HfO₂ with high remanent polarization and long endurance have been demonstrated.

1. Introduction

Two-dimensional (2D) materials are layered crystals with strong in-plane covalent bonds and weak interlayer van der Waals bonds [1-3]. These materials have many unique chemical, mechanical, optical and electrical properties, which not only provide a platform to

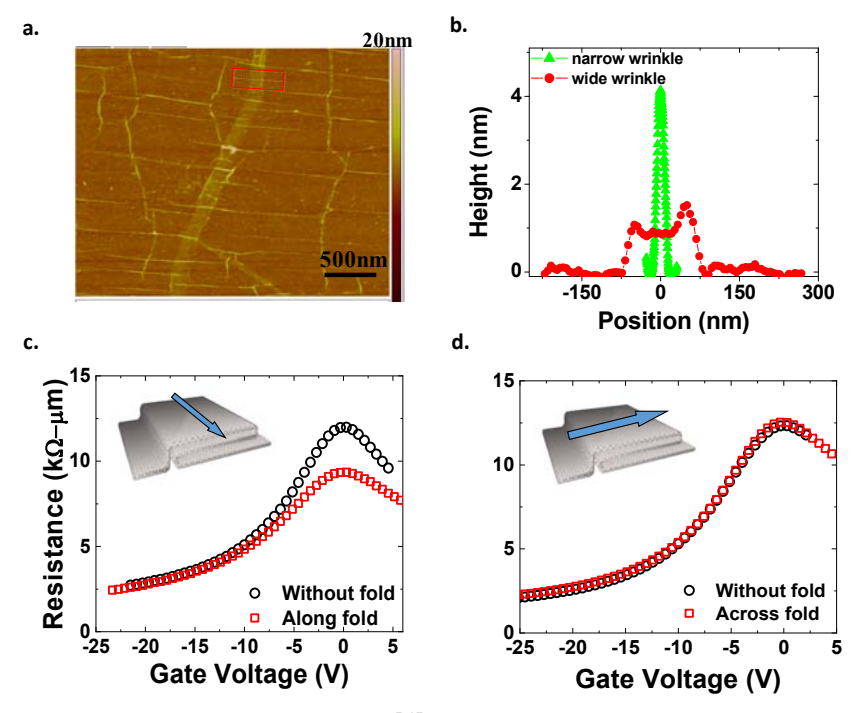


Figure 1. Electronic transport in graphene wrinkles [4]. (a) AFM image of graphene on SiO₂/Si substrate. The field of view is 3 μm. (b) The step profile of a wide and a narrow wrinkle. (c) Averaged resistances as a function of gate voltage for devices along the fold, compared with the control devices without fold. (d) Averaged resistances as a function of gate voltage for devices across the fold, compared with the control devices without fold.

investigate fundamental physical phenomena but also enable novel devices and systems for potential technological applications [6-15]. In this work, we studied the electrical properties of graphene and transition metal dichalcogenides (TMDs), and explored the nano-scale electronic/photonic devices based on these materials.

A ferroelectric dielectric is a polar dielectric in which the polarization can be switched between two or more stable states by the application of an electric field. Traditional ferroelectric materials are primarily complex perovskites, such as lead zirconate titanate (PZT), strontium bismuth tantalate (SBT), and lead magnesium niobate-lead titanate (PMN-PT) [17, 18]. However, these traditional ferroelectric materials have limited thickness scaling and are not compatible with CMOS processes, making them difficult to be adopted in the semiconductor industry. In the last few years, doped HfO₂ has emerged as a new class of ferroelectric material [19-21]. The advantages of the HfO₂-based ferroelectrics include excellent scalability, high coercive field, long retention, and full compatibility with CMOS processes [22-24]. In this work, we investigated aluminum (Al) doped HfO2 as a ferroelectric material for memory applications.

2. Discussion

2.1 Graphene

We have systematically studied the electrical transport in graphene obtained by exfoliation, chemical vapor deposition, and epitaxial growth. We found that the temperature and carrier density dependencies of carrier mobility in monolayer and bi-/tri-layer graphene are diametrically opposite. This fact can be ascribed to the different density-of-states in monolayer and bi-/tri-layer graphene and the screening effect [25]. The morphology also plays an important role in the current transport of graphene. We found that graphene wrinkles can induce local anisotropic conductance. The average resistance of the device along the fold is smaller than that without the fold, especially when biased near the charge neutrality point. The average resistance of the device across the fold is slightly higher than that without fold, shown in Fig.1c-1d [4]. This anisotropy can be attributed to the fact that transport along and across the folded wrinkles are limited by different mechanism: diffusive transport of the charge distributed across the multilayered folds, versus local interlayer tunneling across the collapsed region. Graphene possesses high potential in RF devices due to its ultra-high carrier successfully mobility. We have demonstrated

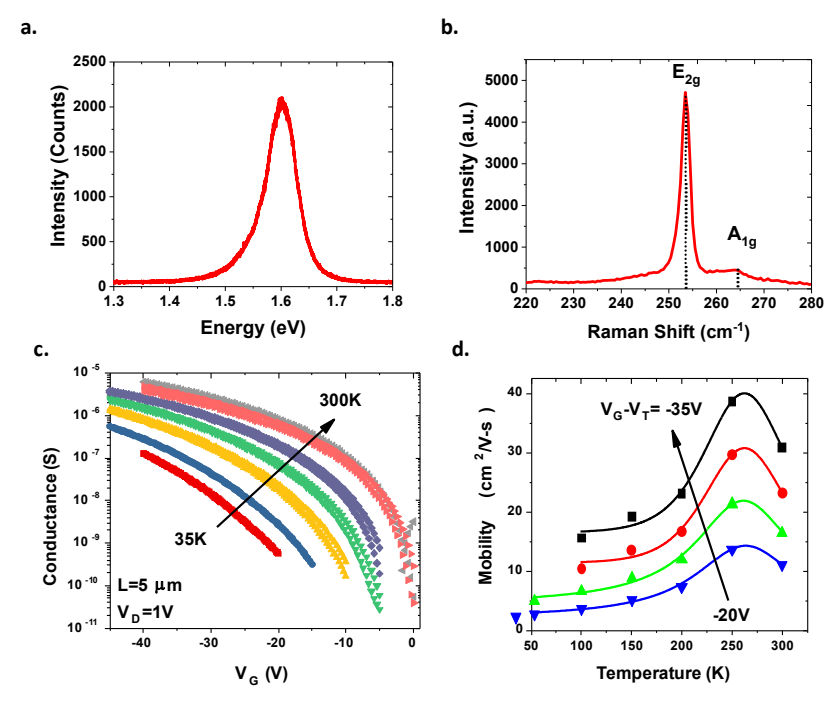


Figure 2. Monolayer WSe₂ grown by CVD. (a) Photoluminescence spectrum and (b) Raman spectrum of synthesized WSe₂. (c) Four-point conductance as a function of gate voltage measured at various temperatures. (d) Temperature dependence of the field-effect mobility at various gate overdrives. [5]

high-frequency graphene RF devices on both rigid substrates and flexible polyimides [26, 27].

2.2 Transition Metal Dichalcogenides

Beyond graphene, TMDCs emerged in recent years as a new group of 2D materials. TMDCs are van der Waals materials with the chemical formula of MX₂, where M is a transition metal atom (such as Mo, W, Hf, or Zr) and X is a chalcogen atom (S, Se, or Te). One layer of M atoms is sandwiched between two layers of X atoms. Unlike graphene which has zero bandgap, most TMDCs have sizable bandgap, which makes them potentially suitable for logic applications.

We have systematically investigated the synthesis of MoS2 and WSe2 using CVD. We found that the hydrogen flow rate and the amount of tungsten oxide (WO₃) precursor can significantly influence the morphology of the WSe₂ [5]. Monolayer MoS₂ and WSe₂ with domain size up to 100 μm were synthesized on SiO₂/Si substrates. Fig. 2a-2b show the typical photoluminescence (PL) and Raman spectra of the synthesized WSe₂. Bright light emission at ~1.60 eV and symmetric single PL peak suggest the direct bandgap nature of monolayer WSe2. The Raman and the atomic force microscopy (AFM) measurements confirm that it is monolayer WSe2. The conductance of WSe2 was tested at various temperatures, shown in Fig. 2c. We found that the hole mobility of the monolayer WSe2 is limited by Coulomb scattering below 250 K, while it is limited by phonon scattering above 250 K (Fig. 2d) [5].

For traditional CMOS devices based on silicon, one key challenge in device scaling is the short-channel effect. To enhance the gate control and suppress the short-channel effect, reducing the thickness of the channel is required. In this regard, thinner silicon has been pursued by using SOI (silicon-on-insulator) and ETSOI (extremely thin silicon-on-insulator). However, the mobility degrades markedly as the thickness is scaled down due to surface roughness. Atomically thin 2D semiconducting material such as MoS₂ and WSe₂ can address this problem. We fabricated logic devices based on MoS₂ with various channel lengths from 4 µm to 32 nm. Despite the thick dielectric, a clear upturn of drain-induced barrier lowering (DIBL) is only observed at a channel length of 32 nm, shown in Fig. 3b. Extrapolating to a device with a 3 nm HfO₂ gate insulator would predict a limiting channel length feature of 7 nm. These results suggest that MoS₂ could be a very promising material for scaled, high-density electronics [16].

The gap states in MoS₂ were characterized using alternative current (AC) conductance and multi-frequency C-V methods (Fig. 3c) [16]. Based on the density of the interface states, we can estimate the number of carriers trapped in the localized states and mobile carriers in the conduction band. We found that the true band mobility is significantly higher than the

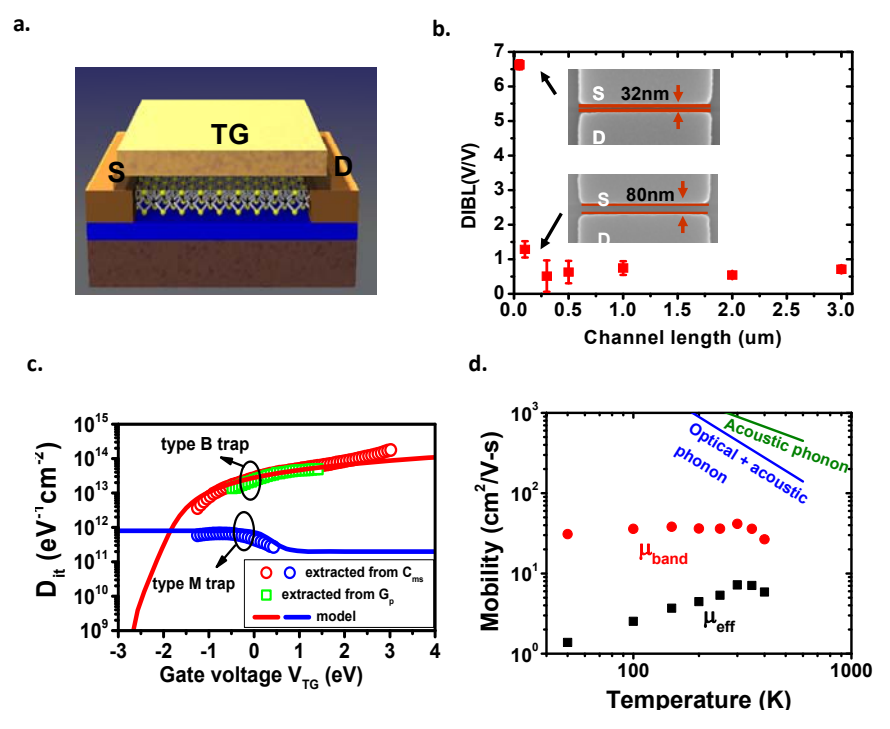


Figure 3. (a) Schematic of MOSFET with monolayer MoS₂. (b) Drain-induced barrier lowering (DIBL) of MOSFET with CVD MoS₂ at various channel lengths. The insets show SEM images of the 32 and 80 nm channel length devices. (c) Density and time constant of trap states as a function of gate voltage. The symbols are experimental results extracted from the capacitance and ac conductance. The lines are models. (d) Effective mobility and corresponding band mobility as a function of temperature. [16]

measured effective mobility due to the large number of gap states in the MoS₂ grown by chemical vapor deposition (CVD), shown in Fig. 3d [16].

2.3 Ferroelectric Doped Hafnium Oxide

We investigated Al-doped HfO_2 with various annealing temperatures, compositions, and metal electrodes [28]. With optimized process conditions, we demonstrated high-performance ferroelectric Al-doped HfO_2 capacitors with remanent polarization over 15 μ C/cm², endurance higher than 10^8 cycles, and retention over 10 years [28]. We envision that ferroelectric-doped HfO_2 will have broad applications in ferroelectric random access memories, negative capacitance field-effect transistors, ferroelectric tunneling junctions, and piezoelectric devices.

3. Summary

Our studies revealed that the current transport in graphene is highly influenced by the number of layers and local topography. High-frequency RF devices based on graphene have been demonstrated. Large-area MoS₂ and WSe₂ were synthesized and logic devices based on monolayer MoS₂ show great potential to suppress short-channel effects and extend the device scaling. Ferroelectric Al-doped HfO₂ devices with high polarization were demonstrated. These new materials and devices will have broad applications in computing, communication, biology, and medicine.

4. Acknowledgments

The authors would like to acknowledge the support from the National Science Foundation (NSF) under grants ECCS 16-11279 and ECCS 16-53241 CAR.

References

- [1] K. S. Novoselov et al., Proceedings of the National Academy of Sciences of the United States of America, vol. 102, no. 30, pp. 10451-10453, Jul 26 2005.
- [2] M. Chhowalla, H. S. Shin, G. Eda, L. J. Li, K. P. Loh, and H. Zhang, *Nature Chemistry*, vol. 5, no. 4, pp. 263-275, Apr 2013.
- [3] K. J. Koski and Y. Cui, *ACS Nano*, vol. 7, no. 5, pp. 3739-3743, 2013/05/28 2013.
- [4] Y. Q. Wu et al., Acs Nano, vol. 6, no. 3, pp. 2610-2616, Mar 2012.
- [5] Z. H. Yao, J. L. Liu, K. Xu, E. K. C. Chow, and W. J. Zhu, *Scientific Reports*, vol. 8, Mar 27 2018.
- [6] G. Fiori *et al.*, *Nature Nanotechnology*, vol. 9, no. 10, pp. 768-779, Oct 2014.
- [7] Q. H. Wang, K. Kalantar-Zadeh, A. Kis, J. N. Coleman, and M. S. Strano, *Nature Nanotechnology*, vol. 7, no. 11, pp. 699-712, Nov 2012.
- [8] A. K. Singh and R. G. Hennig, Applied Physics

- Letters, vol. 105, no. 4, Jul 28 2014.
- [9] J. H. Ahn *et al.*, *Nano Letters*, vol. 15, no. 6, pp. 3703-3708, Jun 2015.
- [10] R. S. Yan et al., Nano Letters, vol. 15, no. 9, pp. 5791-5798, Sep 2015.
- [11] G. Fiori et al., Nature Nanotechnology, vol. 9, no. 12, pp. 1063-1063, Dec 2014.
- [12] D. Jariwala, V. K. Sangwan, L. J. Lauhon, T. J. Marks, and M. C. Hersam, *Acs Nano*, vol. 8, no. 2, pp. 1102-1120, Feb 2014.
- [13] O. V. Yazyev and A. Kis, *Materials Today*, vol. 18, no. 1, pp. 20-30, Jan-Feb 2015.
- [14] R. Cheng et al., Proceedings of the National Academy of Sciences of the United States of America, vol. 109, no. 29, pp. 11588-11592, Jul 17 2012.
- [15] L. K. Li et al., Nature Nanotechnology, vol. 9, no. 5, pp. 372-377, May 2014.
- [16] W. J. Zhu et al., Nature Communications, vol. 5, Jan 2014.
- [17] N. Setter et al., Journal of Applied Physics, vol. 100, no. 10, Nov 15 2006.
- [18] Y. Xu, Ferroelectric Materials and their Applications. Amsterdam: Elsevier, 1991, pp. 1-391.
- [19] S. Mueller *et al.*, *Advanced Functional Materials*, vol. 22, no. 11, pp. 2412-2417, 2012.
- [20] U. Schroeder et al., Japanese Journal of Applied Physics, vol. 53, no. 8, pp. 85-89, Aug 2014.
- [21] E. Yurchuk *et al.*, *Ieee Transactions on Electron Devices*, vol. 61, no. 11, pp. 3699-3706, Nov 2014.
- [22] E. Yurchuk *et al.*, *Thin Solid Films*, vol. 533, pp. 88-92, Apr 30 2013.
- [23] U. Schroeder et al., Ecs Journal of Solid State Science and Technology, vol. 2, no. 4, pp. N69-N72, 2013.
- [24] A. Chernikova et al., Acs Applied Materials & Interfaces, vol. 8, no. 11, pp. 7232-7237, Mar 23 2016.
- [25] W. J. Zhu, V. Perebeinos, M. Freitag, and P. Avouris, *Physical Review B*, vol. 80, no. 23, Dec 2009.
- [26] W. J. Zhu et al., Applied Physics Letters, vol. 102, no. 23, Jun 10 2013.
- [27] W. J. Zhu, T. Low, D. B. Farmer, K. Jenkins, B. Ek, and P. Avouris, *Journal of Applied Physics*, vol. 114, no. 4, Jul 28 2013.
- [28] H. Ryu, K. Xu, J. Guo, and W. Zhu, 76th Device Research Conference Santa Barbara, California, 2018.